J ournal of Economics , Technology , and Business (JETBUS)
Volume 3 , Number 12 December 2024
p-ISSN 2964-903X; e-ISSN 2962-9330

Introduction to The Earth Field In Bukit Batu Putih, Samarinda City, East Kalimantan

Hamzah Sidik[1], Rio Syaputra SN[2], Vannes[3], Jimmy Fernandez[3], Yusnul[3], Wira Kusuma[4], Ibnu Amzad Rizqulloh[5]
Universitas Kutai Kartanegara, Indonesia
Email: hamzahsidik86@gmail.com
Correspondence: hamzahsidik86@gmail.com

KEYWORDS:
Limestone, White Stone Hill, mining, geological formation of Balang Island, environmental management.

ABSTRACT

This Introduction to Earth Science Field Lecture activity was conducted at Bukit Batu Putih, Samarinda City, which is the Balang Island Formation (Tmpb). This location was chosen because of the dominance of limestone in the area and the significant limestone mining activities. This study aims to understand the local geological characteristics, identify limestone types, and analyze the impact of mining on the surrounding environment. The methodology used in this study includes field observation, geological mapping, and visual analysis and limestone sample assessment. Field observations were conducted to identify the structure and texture of limestone and geological formations around the location. Geological mapping was conducted to map the distribution of limestone and understand the stratigraphic relationship between rock layers. The results of the study indicate that limestone consists of clastic and fossiliferous limestone types, which are formed from calcium carbonate deposits. Mining activities in this area have revealed many limestone layers that have economic potential. However, mining also has environmental impacts, such as changes in land morphology and degradation of water quality. The conclusion of this study emphasizes the importance of understanding regional geology and limestone characteristics for better resource management. Recommendations are provided for improving environmentally friendly mining practices and conservation efforts to maintain the balance of the ecosystem in Bukit Batu Putih.

INTRODUCTION

Indonesia, as a country with abundant natural resources, faces considerable challenges related to environmental sustainability. In the context of rapid economic growth, exploitation of natural resources is often carried out without considering the long-term impacts on ecosystems (Barbier, 2019; Putra et al., 2023; Saleh et al., 2020). Global issues, such as climate change, deforestation and environmental pollution, show alarming trends and require serious attention. According to a report by the Central Bureau of Statistics, forest loss reaches around 2.5 million hectares per year, mostly due to mining and agricultural activities. In this case, the issue of mineral resource exploitation becomes very relevant, especially in the context of its impact on ecosystem balance (Lu & Zhao, 2024).

The Bukit Batu Putih area in Samarinda, East Kalimantan, is one of the areas directly affected by intensive mining activities, particularly limestone mining. The area, which is part of the Balang Island Formation, not only has high mineral resource potential, but has also experienced significant impacts on the environment. Specific problems that arise include changes in land morphology, degradation of water quality, and negative impacts on biodiversity (Issaka & Ashraf, 2017). Unplanned mining can cause erosion, sedimentation, and water pollution that ultimately threaten public health and the sustainability of natural resources in the area.

A number of previous studies have been conducted to explore the environmental impacts of mining activities in various locations in Indonesia. However, research specifically focusing on Bukit Batu Putih is still very limited. Existing studies tend not to provide a comprehensive picture of the impact of mining on the environment and resource potential in the area. For example, Ahmad et al.'s (2020) study showed that limestone mining in other areas resulted in significant changes to soil and water quality, but did not adequately address the geological characteristics and economic potential that could be explored in the Bukit Batu Putih area.

The urgency of this research is very high, given the importance of maintaining a balance between natural resource exploitation and environmental preservation. With the increasing demand for mineral resources, there is an urgent need for researchers and decision makers to understand the implications of mining activities in order to develop more sustainable practices. This research aims to provide the necessary information to support better decision-making in resource management in Bukit Batu Putih. In addition, the results of this study are expected to contribute to environmental conservation efforts and the protection of the rights of local communities affected by mining activities.

The novelty of this research lies in the integrative approach that combines geological analysis, environmental impacts, and economic potential in one study. The methodology used includes field observations, geological mapping, and a more systematic evaluation of environmental impacts. Using this approach, the research will not only answer questions relating to geological characteristics and mining impacts, but will also provide recommendations for more sustainable management practices. This research seeks to provide a deeper understanding of the interactions between mining activities and the environment, and their impact on the quality of life of local communities.

This research aims to identify and analyze the geological characteristics of the Bukit Batu Putih area, as well as evaluate the impact of mining on the environment. As such, this research is expected to contribute to the development of better policies for mineral resource management and environmental protection in Bukit Batu Putih.

RESEARCH METHOD

Research in Bukit Batu Putih, Samarinda City, uses various methods to obtain accurate and comprehensive data on the geological conditions of the area. The research methods used include, Primary Data Collection and Secondary Data Collection. Primary data collection is carried out through direct observation in the field using the following techniques, 1) Geomorphological Mapping. 2) Observation and Sampling of Rocks. 3) Analysis of River Flow Patterns. 4) Survey of Mining Potential. Secondary Data Collection, Secondary data collection is carried out by collecting information from various sources of literature and existing data, 1) Literature Study, 2) Government and Institutional Data. Data Analysis, data obtained from the field and secondary sources are analyzed using several analysis techniques. 1) Geomorphological Analysis, 2) Stratigraphic Analysis, 3) River Flow Pattern Analysis, 4) Evaluation of Mining Potential.

RESULTS AND DISCUSSION

Basic Image and Geomorphology of the Research Area

The study of basic imagery and geomorphology in Bukit Batu Putih, Samarinda, aims to understand the topographic forms and patterns as well as the dominant geomorphic processes in the area. The importance of this study lies in the preparation of geomorphological maps, identification of potential georisks such as erosion and landslides, and its support in environmental conservation, spatial planning, and natural resource management (Morino et al., 2022; Wang & Nanehkaran, 2024; Youssef et al., 2021). Information from this study also helps in monitoring environmental changes and sustainable decision-making related to development and environmental protection in Bukit Batu Putih.

Data and Methodology

There are two types of data used as base maps to conduct this research. Before the field study was conducted, the data used as base maps were satellite imagery and DEMNAS topography. While in the field study process, orthophoto data acquisition using *drones* was carried out so that data was obtained in the form of *orthomosaic* and *dense cloud* / *point cloud* which were then processed into topographic data in the form of surface models and then reprocessed into *terrain* models. *The surface* model itself is a surface model that still includes trees, buildings and whatever is on the ground surface when data acquisition with *drones* is carried out, *post-processing* of data to become *a terrain* model is carried out to separate objects other than the ground in order to obtain a land surface model only (Green et al., 2019; Pessacg et al., 2022).

Topographic Data and Satellite Imagery (DEMNAS)

As stated in the previous section, the topographic data used before the field study was DEMNAS data with the code 1915-41_v1.0. This data was obtained from the Geospatial Information Agency via the internet/ official *website* of the DEMNAS data provider and national *bathymetry* . The research area in question is in sheet 1915-41_v1.0 on the DEMNAS map index. The National DEM was constructed from several data sources including IFSAR data (5m resolution), TERRASAR-X (5m *resampling resolution* from the original resolution of 5-10 m) and ALOS PALSAR (11.25 m resolution), by adding *mass point data* used in making the Indonesian Topographic Map (RBI). The spatial resolution of DEMNAS is 0.27-arcsecond, using the EGM2008 vertical datum.

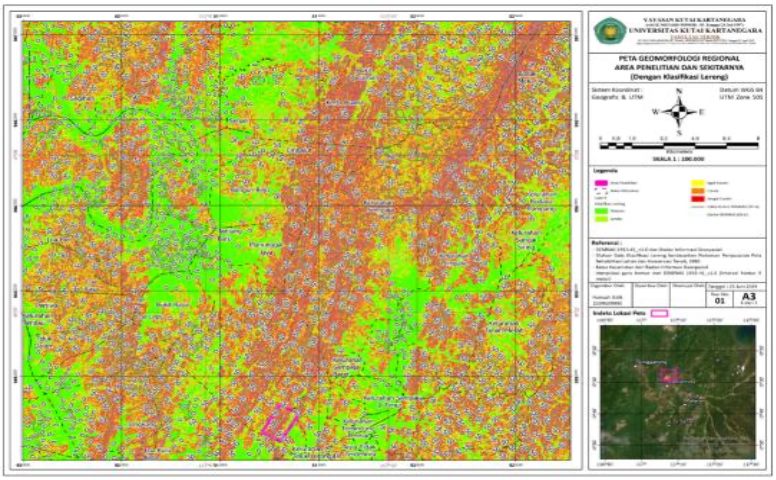

Figure 1. Geomorphological Map of DEMNAS 1915-41_v1.0 with slope classification

masspoint data into *Digital Surface Model* /DSM (IFSAR, TERASAR-X or ALOS-PALSAR) using *GMT-surface* with *tension* 0.32. Details of the assimilation process can seen in the IHO-GEBCO Bathymetry Cookbook.

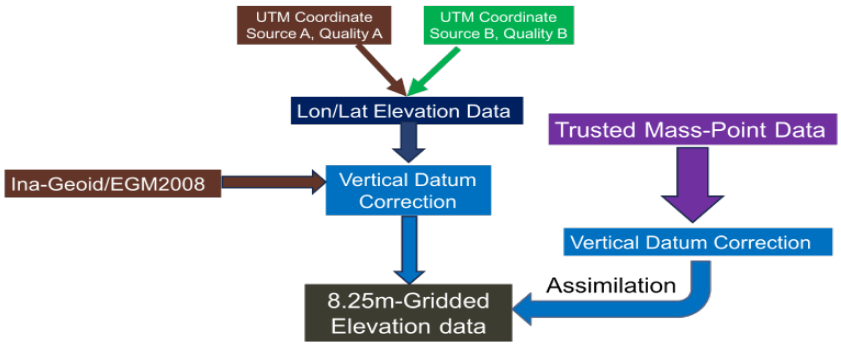

Figure 2 . DEM processing flowchart

Ground Control Point (GCP) and Geodetic Control Network (GKN) measurements are used for validation and accuracy testing of DEMNAS data and other height data models. The validation results in Sumatra show that the accuracy of DEMNAS is better than the height data model formed from *masspoint* , *spotheight* and *breakline* (hereinafter referred to as DTM). DEMNAS, DTM and DSM data (IFSAR, TERRASAR-X and ALOS-PALSAR) for the Sumatra region (for other regions, the graph is not shown) have *Root Mean Square Error* (RMSE) of 2.79m, 3.24m and 3.71m respectively with bias *errors* of -0.13m, -0.63m and 2.21m for DEMNAS, DTM and DSM data.

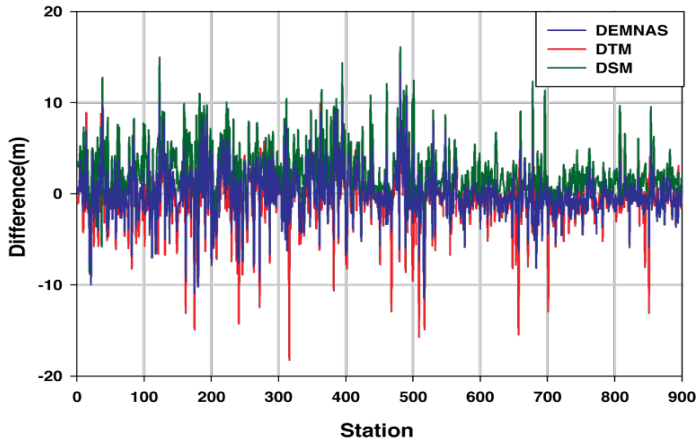

Figure 3. Difference between GCP/JKG minus EGM2008 and height data model

The difference in GNSS and DEMNAS measurement values does not have a directly proportional relationship with the measured elevation. This height difference may be more due to land cover than elevation height. The relationship between the DEMNAS and GNSS differences can be seen in the following graph.

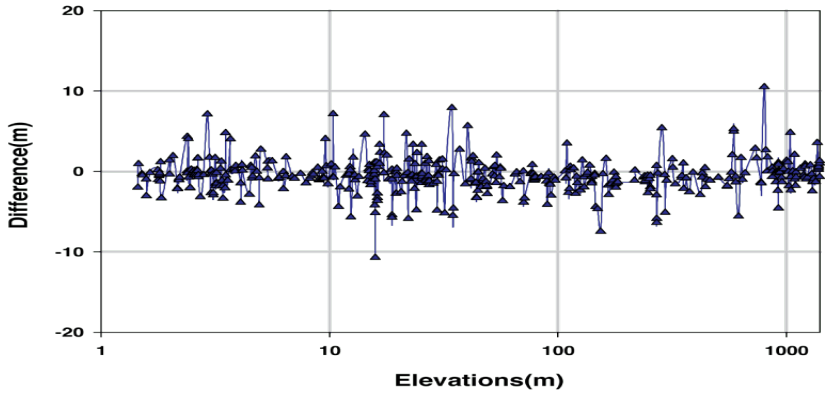

Figure 4. Relationship between the difference between DEMNAS and GNSS and elevation height

In terms of accuracy, DTM built from *masspoints* and *breaklines* has good accuracy for drawing contour lines on maps. However, in certain relatively extreme cases, creating DTM from *masspoints* and *breaklines* can change *the landscape* of the area. This *landscape change* is caused by the low accuracy *of masspoints* and *breaklines* both in terms of horizontal and vertical positions, resulting in a higher DTM than DSM, and changes in river features in several places (image below). On the other hand, the process of adding *masspoint data* to DSM uses *GMT-surface* with *boxcar The filter* produces higher quality data, by removing inaccurate *masspoints.*

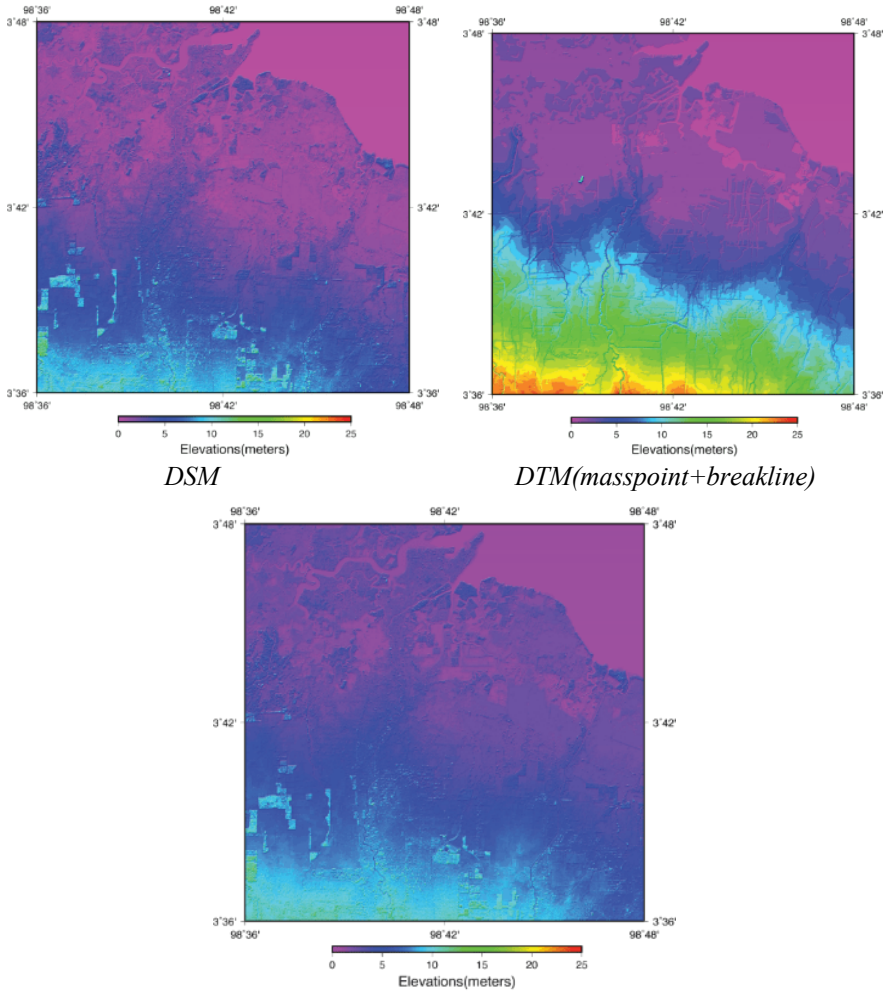

DSM *DTM(masspoint+breakline)*

DEMNAS

Figure 5. Comparison of DSM, DTM (*Maspoint* + *Berakline*) and DEMNAS *Processing*

The effect of the height datum conversion from EGM96 to EGM2008 is seen in DSM which still uses EGM96 and DEMNAS which refers to EGM2008. Furthermore, height anomalies are also seen in DTM data obtained from *masspoints* and *breaklines from stereo-plotting* interpretation results in the southern area, with DTM data higher than DSM, 10 m or more. Other landform anomalies are also seen in the flow pattern and river mouths in the northern part. The released DEMNAS data is cut according to the Map Sheet Number (NLP) scale 1:50k or 1:25k, for each Island or Archipelago. A summary of the DEMNAS characteristic data set, as follows:

Table 1. Summary of DEMNAS characteristics data set

Item	Description
File Name	DEMNAS_xxxx.yy-v1.0 tif for N.P. 150k and DEMNAS.xyy-v1.0 tif for 125k: xxxx.yy indicates the map sheet number from RBI, and v1.0 indicates version 1.0
Resolution	0.27-arcsecond
Datum	EGM2008
Coordinate System	Geographic
Format	Geotiff 32bit float

Seamles data with a wider area, *the Geospatial Data Abstraction Library can be used (GDAL)*. Here is an example of merging data with GDAL using the terminal. Merging 10 (ten) NLP DEMNAS data only takes 5 seconds, with the following instructions:

```
[kebo@tides SAMPLE]$ ls
DEMNAS_1314-23.tif DEMNAS_1314-31.tif DEMNAS_1314-34.tif DEMNAS_1314-61.tif
DEMNAS_1314-63.tif
DEMNAS_1314-24.tif DEMNAS_1314-33.tif DEMNAS_1314-52.tif DEMNAS_1314-62.tif
DEMNAS_1314-64.tif
[ kebo@tides SAMPLE]$ echo "gdal_merge.py -o DEMNAS_large_area.tif " > list1
[ kebo@tides SAMPLE]$ ls DEMNAS_*. tif | tr -d ' \n ' | sed -e 's/. tif /. tif /g' > list2
[ kebo@tides SAMPLE]$ paste list1 list2 > command.sh
[ kebo@tides SAMPLE]$ sh command.sh
0...10...20...30...40...50...60...70...80...90...100 - done.
```

Plotting DEMNAS data can done with *Generic Mapping Tool (GMT)* and GDAL for data conversion from GeoTiff become NetCDF . As example , usage *bourne -shell script* simple (*plot_demnas.bash*) with order as following :

```
bash-3.2$ bash plot_demnas.bash
 usage : bash plot_demnas.bash file_input.tif output_file.eps max_elev (meters)
 example : bash plot_demnas.bash DEMNAS_0718-54_v1.0.tif DEMNAS_0718-54_v1.0.eps
200
bash-3.2$ bash plot_demnas.bash DEMNAS_0718-54_v1.0.tif DEMNAS_0718-54_v1.0.eps
15
Input file size is 3333, 3333
0...10...20...30...40...50...60...70...80...90...100 - done.
grd2cpt: Processing input grid(s)
grd2cpt: Mean and SD of data are 4.1996872704 2.81747693968
grdgradient: Processing grid input
grdgradient: Min Mean Max sigma intensities:grdgradient: -0.511577595155
9.02550576079e-05 0.53745034241 0.0418320305703
grdhisteq: Processing grid input
```

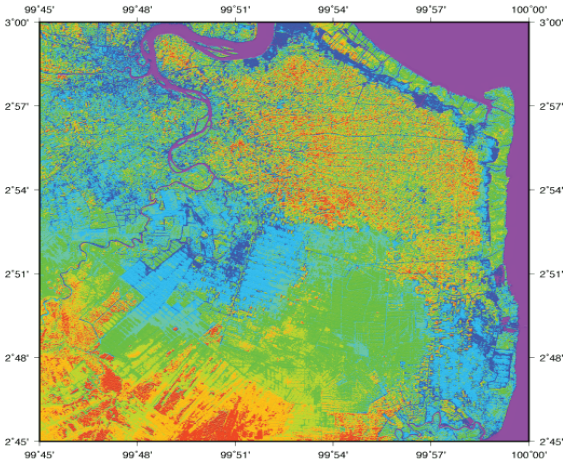

Figure 6. Plotting results with GMT

The height datum used in DEMNAS is EGM2008. If you want to use another height datum, for example the mathematical field of Elipsoid, MSL or others, you can use CDO to *regrid* the height datum data according to the NLP cut of DEMNAS data, or directly use *the command-line tools* in GDAL. The following is an example of using *the command-line tools* (conv2ellipsoid.bash) in GDAL to restore the height datum from EGM2008 to the ellipsoid.

```
bash-3.2$ bash conv2ellipsoid.bash
 usage : bash conv2ellipsoid.bash file_input.tif file_output.tif
 example : bash conv2ellipsoid.bash DEMNAS_0718-54_v1.0.tif DEMNAS_EL_0718-54_v1.0.tif
bash-3.2$ bash conv2ellipsoid.bash DEMNAS_0718-54_v1.0.tif DEMNAS_EL_0718-54_v1.0.tif
Input file size is 4201, 3001
0...10...20...30...40...50...60...70...80...90...100 - done.
```

0 .. 10 .. 20 .. 30 .. 40 .. 50 .. 60 .. 70 .. 80 .. 90 .. 100 – Done

Data Collection Using Drones

In the process of acquiring orthophoto data using *drone* various *quadcopter* . *Drones* used is the DJI Mavic Pro Platinum without modification (standard). Although No type *high end drone* or type latest, will but *DJI Mavic Pro Platinum Drone* is one of device yes Enough adequate in technology *drone* moment this, which offers good combination between portability, capability, and quality results recording. This *drone* is designed with various advanced features that allow users to take high-quality aerial photos and videos and run various surveying and mapping applications with high efficiency.

Table 2. DJI Mavic Pro Platinum Specifications

Feature	Specification
Heavy	734 grams (including battery and propeller)
Size	Folded : 83mm x 83mm x 198mm Open: 83mm x 198mm x 83mm (without propeller)
Camera	Sensor : 1/2.3” CMOS Photo Resolution : 12.35 megapixels (total pixels: 12.71M) Video Resolution : - C4K : 4096×2160 24p - 4K : 3840×2160 24/25/30p - 2.7K : 2704×1520 24/25/30p - FHD : 1920×1080 24/25/30/48/50/60/96p - HD : 1280×720 24/25/30/48/50/60/120p

	- Photo Format : JPEG, DNG (RAW) - Video Format : MP4, MOV (MPEG-4 AVC/H.264)
Dreadlocks	3-axis (tilt, roll, pan)
Maximum Flight Distance	7 km (without obstacles , interference)
Flight Time	About 30 minutes (no wind and constant speed of 25 kph)
Speed Maximum	65 kph (in Sport Mode without wind)
System Navigation	GPS + GLONASS
Battery	3,830 mAh LiPo 3S
Key Features	- *Obstacle Avoidance* (Avoidance) Obstacle) - *ActiveTrack* (Tracking) Object) - *TapFly* (Navigation via tap on the screen) - *Gesture Mode* (Control via hand movements) - *Return to Home* (Back to Home) point beginning in a way automatic) - *FlightAutonomy* (Autonomous navigation with sensors)

Technology Used

a. Camera Sensor:

The camera with 1/2.3" CMOS sensor enables high-quality stills and video capture. RAW (DNG) format provides flexibility in the editing process.

b. 3-axis Gimbal System:

The 3-axis gimbal ensures camera stability while flying, reducing shake and producing smooth footage.

c. GPS and GLONASS:

Using two satellite navigation systems (GPS and GLONASS) to determine accurate and stable position during flight.

d. *Obstacle Avoidance* :

This technology uses sensors to detect and avoid obstacles in the *drone's flight path* , preventing collisions and improving flight safety.

e. *ActiveTrack* and *TapFly* :

- *ActiveTrack* feature allows *the drone* to follow and record moving objects automatically.
- *TapFly* allows users to determine flight paths simply by tapping a point on the phone or tablet screen.

f. *Gesture Mode* :

Allows users to take photos or videos through hand gestures, without the need to operate *a remote control.*

g. *Return to Home (RTH):*

The drone automatically returns to the flight starting point when the battery is low or if it loses signal.

To obtain optimal results in aerial photography or mapping, the flight altitude depends greatly on the specific purpose of the flight:

a. Photography and Videography:

Flying altitudes between 50-120 meters are usually ideal for capturing wide views and good detail.

b. Mapping and Surveying:

Flight altitude can vary depending on the desired resolution. Typically, altitudes between 60-100 meters provide optimal results with sufficient detail for mapping purposes.

c. Obstacle Avoidance:

Given the *obstacle avoidance feature*, maintaining a higher altitude can help avoid obstacles such as trees or tall buildings.

The data collection process in the field begins with planning the flight path, ensuring that the sky conditions and the *take-off* and landing location/position are safe or free from interference/obstacles either on land or in the air up to a certain height, weather, and so on.

Figure 7 . Flight Path Plan

Before orthophoto data acquisition, a flight path plan was created using the trial version of the *DroneDeploy application. In addition to DroneDeploy*, several other applications can also be installed on the controller (via *mobile phone*) for automatic flight. Based on the author's experience, this automatic flight method is safer and more precise than manual flight. Another step before performing orthophoto data acquisition is to install *ground control points* in the field that are *the area of interest* for measurement. *Ground control points* are installed at strategic points that are open and clearly visible from a certain height to be used as references or tie points on the ground during the data acquisition and orthophoto processing process.

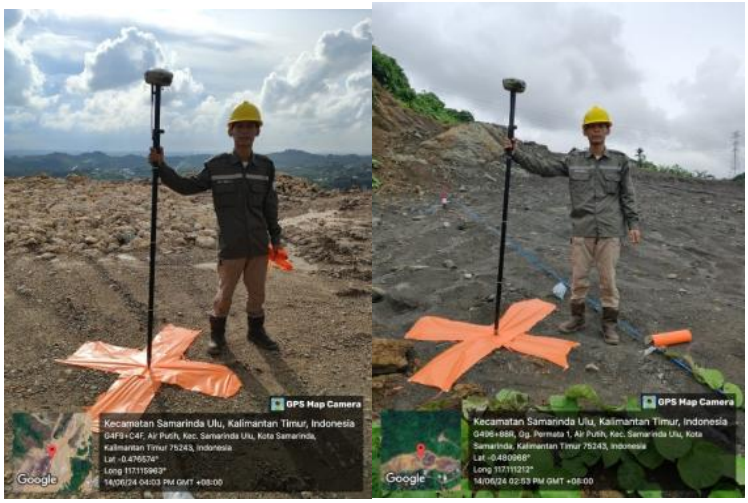

Figure 8. Documentation of *Ground Control Points* at the research location

After *the ground control point* is installed and its coordinates are taken using GPS RTK (*Real Time Kinematic*) / *Geodetic*, the flight for orthophoto data acquisition is almost ready to be carried out, after previously observing the flight area. The acquisition of *Ground Control Point coordinates* is carried out using GPS RTK because it is effective and more practical to use when compared to a total station. In the research conducted, no installation and observation of *benchmark coordinates was carried out*, although the coordinates used were global coordinates (UTM 50S / WGS84). This is because it uses the CORS method

which utilizes the internet network and the nearest CORS station. The CORS station used is in the Samarinda Seberang area with the code CSAM, the location of the *CORS station* can be seen in the following image.

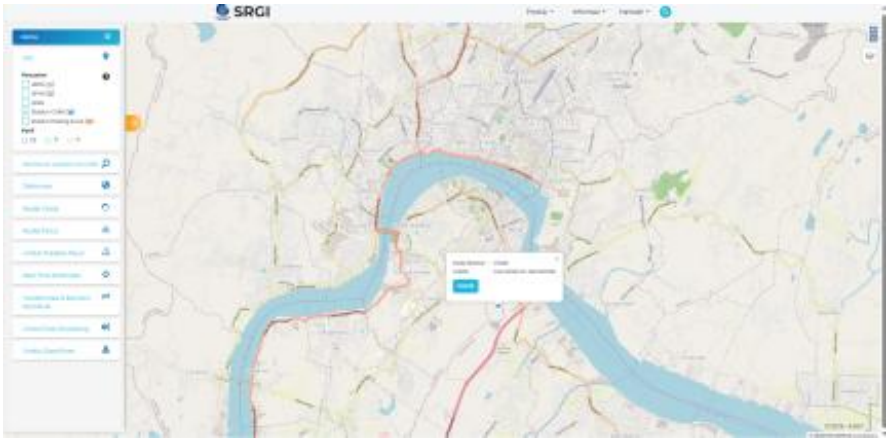

Figure 9. Location of CORS CSAM Station

The observation location is within the radius of the CORS CSAM station (less than 30 km). So the network/signal obtained is quite good with the status *"fixed"* .

Figure 10 . CORS CSAM Station Office

Figure 11. *Receiver* and *Indoor Equipment of* CORS CSAM *Station*

BADAN INFORMASI GEOSPASIAL (BIG)

CSAM

DESKRIPSI STASIUN CORS			
Kode Stasiun	CSAM	Nama Stasiun	Samarinda
Desa/Kelurahan	Rapak Dalam	Kabupaten/Kota	Samarinda
Kecamatan	Loa Janan Ilir	Provinsi	Kalimantan Timur
Lintang	-0.53755235896005	Bujur	117.14635213207
Uraian lokasi	Pilar berada di halaman Stasiun Transmisi TVRI Kalimantan Timur. Stasiun Transmisi TVRI Kalimantan Timur, Kota Samarinda		
KOORDINAT DAN LAJU KECEPATAN STASIUN CORS			
Koordinat Kartesian (SRGI2013)		Koordinat Geodetik	
X	-2910080,240 meter	Lintang	0 ° 32' 15,18849" S
Y	5675468,712 meter	Bujur	117 ° 8' 46,86768" E
Z	-59440,401 meter	Tinggi Ellipsoid (h)	191,076 meter
Kecepatan Pergeseran Kartesian		Kecepatan Pergeseran Toposentrik	
Vx	-0,021 meter/tahun	V utara	-0,011 meter/tahun
Vy	-0,013 meter/tahun	V timur	0,024 meter/tahun
Vz	-0,011 meter/tahun	V vertikal	-0,002 meter/tahun
PERANGKAT			
Receiver	LEICA GR50	Redome	LEIM
Antena	LEIAR20	Tinggi Antena	0.096
Tahun Dibangun	2021	Ket. Tinggi Antena	Bottom of Antenna
Komunikasi Data	ONLINE		
FOTO DAN SKETSA			
Foto Bangunan dan TKG		Sketsa Lokasi	
Tanggal Pembaharuan :		Kontrol kualitas oleh Pusat Jaring Kontrol Geodesi dan Geodinamika	

Figure 12. Description CORS CSAM Station

After done taking coordinate *Ground Control Point* , list of coordinates saved For later used in the orthophoto processing process.

Table 3. List of Ground Control Point Coordinates

CODE	NORTH	EAST	ELEVATION
GCP-02	9,946,762,392	512,698,476	149,022
GCP-06	9,947,190,228	513,312,451	75,772
GCP-09	9,948,068,073	513,833,070	66,677
GCP-08A	9,947,976,601	512,942,120	101,263
GCP-05	9,947,579,300	512,562,832	75,183
GCP-03	9,946,837,014	512,370,978	80,541
GCP-04	9,947,323,743	512,899,134	162,159
GCP-05A	9,947,492,013	513,015,926	171,803
GCP-01	9,946,519,219	513,074,213	94.198

Data acquisition process is carried out for two days, because on the day First done Already towards the afternoon, where level radiation the sun and the reflection of the light that has not enough good (*bad reflectance*), so to be continued the next day the day.

Figure 13. Some orthophoto results acquisition

Furthermore a number of Photo the processed use *Agisoft software Metashape* (trial version), documentation / captures screen in the processing process can seen in the picture following.

Figure 14. Location of Ground Control Point

Errors on the Z (vertical) axis are indicated by the color of the ellipse on the map or chart. For example, different colors can indicate different levels of error, such as red for high error and green for low error. Errors on the X and Y (horizontal) axes are indicated by the shape of the ellipse. Longer or narrower ellipses indicate different levels of error in the horizontal direction. The longer the ellipse, the greater the error on the X or Y axis. Estimated locations of GCPs (*Ground Control Points*) are indicated by symbols such as dots or crosses. These dots or crosses indicate the calculated or estimated positions of the GCPs based on the available data.

Table 4. Control Point RMSE

Count	X error (cm)	Y error (cm)	Z error (cm)	XY error (cm)	Total (cm)
9	0.755577	0.995592	1.15755	1.24984	1.70354

Orthophoto processing with Agisoft Metashape *software* is only done up to the stage of creating *dense clouds* . The entire process in Agisoft Metashape is done with the following *processing parameters :*

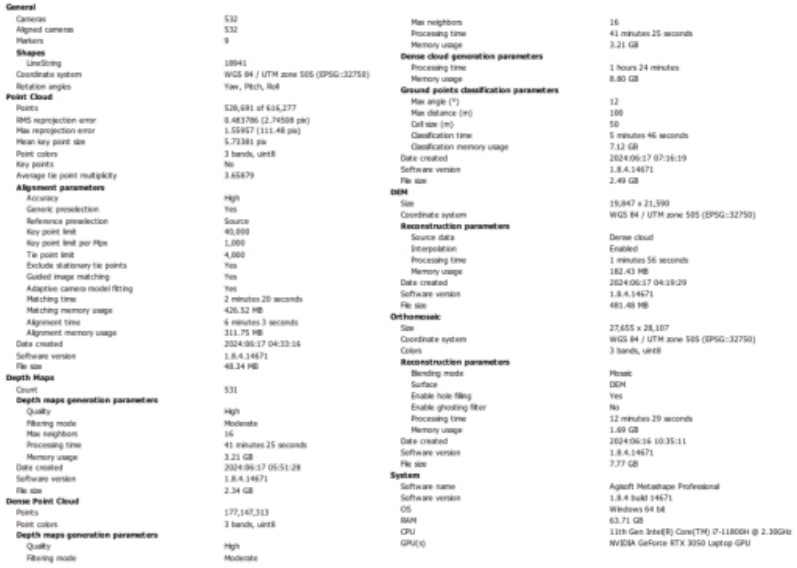

Figure 15. Processing Parameters

Furthermore, to facilitate the process of extracting terrain models from *dense clouds , Quick Terrain Modeller and PCI Geomatica software* are used for calculations and geomatic processes so that the terrain model obtained is smoother and has a more *reliable approach* to actual conditions.

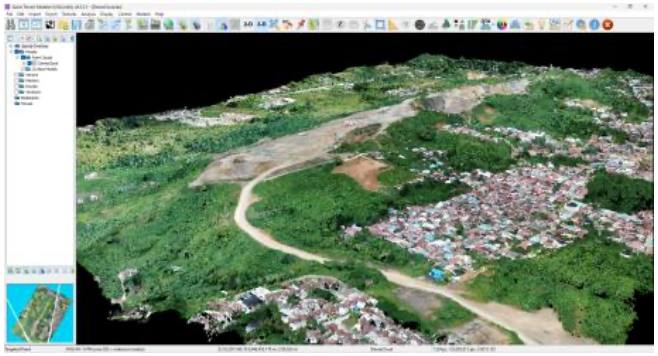

Figure 16 . Dense Cloud view in Quick Terrain Modeller

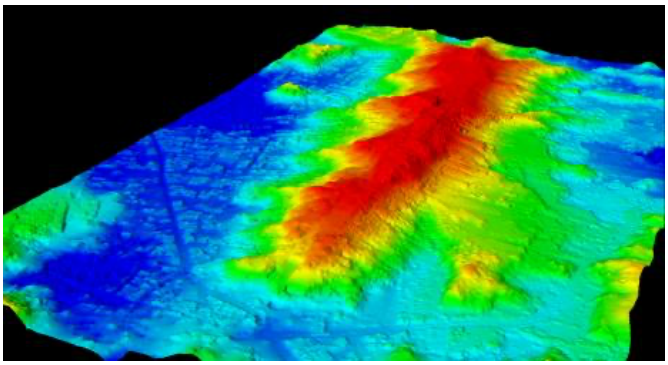

Figure 17. Unfinished Terrain Model smoothing

In figure 17 above can viewed terrain model that has not been in *smoothing*, where Still seen forms rough from settlements and *undulating* on the terrain model that has been made, next done geomatics process for remove the part that is not required like settlements, buildings, *undulating* and the like For get more results specific and only is contour land only. Geomatics process done with PCI Geomatica *software*, *files* from *Quick Terrain Modeler* saved in form *tiff* For processed more continue on PCI Geomatica.

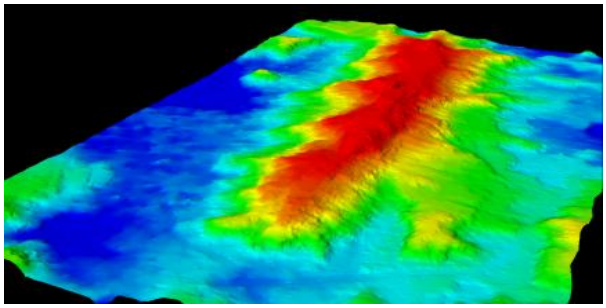

Figure 18. Terrain Model after Geomatics process

Geomorphological Analysis Results

Basic Image of Research Area

The research area is in the DEMNAS 1915-41_v1.0 data index, the position of the white stone hill as the center of the research location is clearly visible.

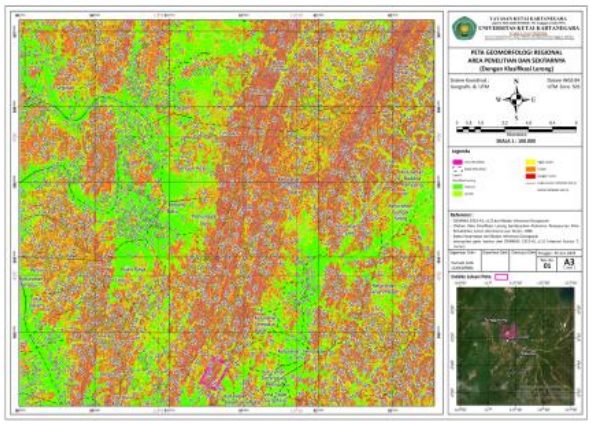

Figure 19. Regional Geomorphology Map of the research area and its surroundings

It can be seen in the image above, more than half of the area in regional geomorphology is dominated by steep to very steep hilly areas, while the rest are plains and gentle hills. Based on geomorphological theory, it can be seen in the image above that more than half of the area in regional geomorphology is dominated by steep to very steep hilly areas, while the rest are plains and gentle hills (Derbyshire, 2019; Huggett & Shuttleworth, 2022). This division shows significant variations in the topography and soil characteristics in the region.

Discussion

Indication of Differences in Rock Hardness and Erosion Levels

Rock Hardness

Rock hardness is an important factor that influences the shape and geomorphological structure of an area. Steep hilly areas are likely to consist of harder rocks that are resistant to weathering and erosion (Goudie, 2016; Hack, 2020; Zondervan et al., 2020). Hard rocks, such as compact limestone and sandstone, tend to form high and steep reliefs because they are resistant to erosion. In contrast, flat and gentle hilly areas may consist of softer rocks, such as sedimentary rocks, which are more easily eroded and form flatter surfaces.

Erosion Rate

The rate of erosion in an area is influenced by a variety of factors, including climate, vegetation, topography, and human activity. Areas with steep slopes tend to experience higher rates of erosion because gravity facilitates the movement of soil and rock material. High rainfall in these areas can also accelerate the erosion process, especially if there is inadequate ground cover vegetation. Vegetation serves to hold the soil and reduce the speed of surface water flow, thereby reducing erosion. When vegetation is reduced, for example due to deforestation, erosion tends to increase.

Factors that Influence

a. Geological Conditions:
   The type and hardness of the rocks in the area affect the formation of topography. Harder rocks will form steeper slopes, while softer rocks will be more easily eroded and form plains (Goudie, 2016).
b. Climate Conditions:
   Heavy rainfall and rainfall intensity can increase erosion rates, especially in areas with steep slopes. Heavy rain can cause landslides and rapid surface flows, transporting soil and rock material (Dikshit et al., 2020; Huang et al., 2024).
c. Vegetation:
   Vegetation acts as an erosion barrier with its roots binding the soil. In areas with dense vegetation, erosion tends to be lower. Conversely, deforestation or reduced vegetation will increase the rate of erosion (Eneh & Nnenwa, 2022).

d. Human Activities:
Development, agriculture, and other human activities can accelerate erosion by changing soil structure and reducing vegetation cover. Unsustainable agricultural practices, for example, can lead to soil degradation and increase erosion (Mujiyo et al., 2021; Rudiarto et al., 2020).

e. Topography:
Land slope greatly affects the rate of erosion. Steep slopes allow water to flow faster, which increases the power of erosion. Gentle plains tend to have lower erosion rates because water flows more slowly (Singh & Hartsch, 2019). The dominance of steep to very steep hills in the study area regionally reflects the complex geological characteristics and erosion processes. The differences in rock hardness and high erosion rates in this region are caused by the interaction of various natural factors and human activities, all of which play an important role in shaping the existing geomorphological landscape.

Detailed Topography from *Drone Data*

To get more specific and current results, re-measurement was carried out using the aerial mapping method using *a drone* tied to *a ground control point* . Several differences can be seen due to changes in hue/land formation due to human work, or other things.

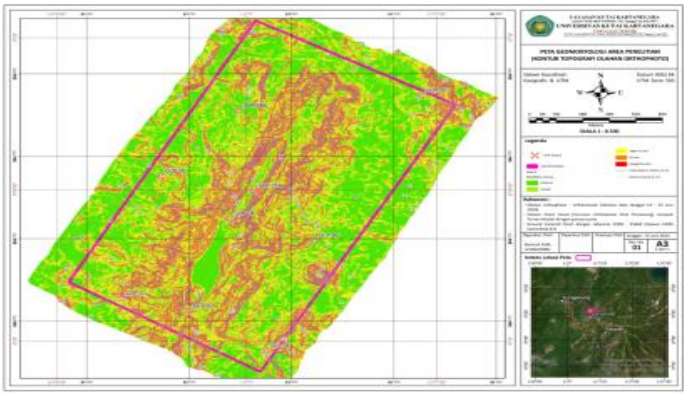

Figure 20. Geomorphological Map of the Research Area (Orthophoto)

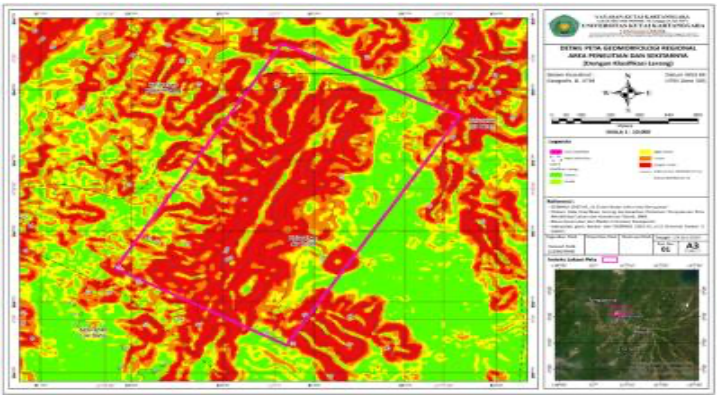

Figure 21. Regional Gemorphology Details of the Research Area

From the two maps above, it is clear that in general the landscape changes, both due to human work (mining, land formation, housing and others) and due to other reasons. If in DEMNAS 1915-41_v1.0 at the top of the white stone hill only left a small area of plains with many steep slopes around it, while based on the results of orthophoto acquisition and terrain model processing, it was found that the plain area at the top of the white stone hill became wider and the steep slopes around it became gentler and some were even relatively flat due to mining activities that had been going on for years in the area.

Some of the potential consequences of this change can be explained as follows:

a. Soil Erosion and Degradation:
   Mining activities that take place over many years can cause increased soil erosion. Steep slopes that have become gentler or flatter due to mining activities can lose their stability, triggering further erosion. This erosion results in soil degradation that can reduce soil fertility and affect agricultural productivity in the surrounding area.
b. Hydrological Changes:
   Topographic changes, especially the reduction of steep slopes to gentler ones, can change water flow patterns. Rainwater that previously flowed quickly on steep slopes can now infiltrate more into the soil on gentler slopes. This can reduce surface runoff and increase the risk of flooding in low-lying areas.
c. Habitat Loss:
   Landscape changes due to mining can cause the loss of natural habitats for local flora and fauna. Areas that were once hilltops with special habitats are now transformed into wider plains, reducing ecosystem diversity and disrupting the balance of nature.
d. Geological Stability:
   Continuous excavation and removal of soil and rock material can disrupt the geological stability of the area. A gentler slope may appear stable, but continued mining activity can cause landslides or ground movement in the future.
e. Microclimate Change:
   Topographic changes can affect the microclimate in an area. Hills and slopes that previously served as windbreaks or temperature regulators may no longer be effective in their roles, which can affect local weather patterns and humidity.
f. Social and Economic Influences:
   Significant changes in the landscape due to human activities such as mining can have an impact on local communities. Land clearing, changes in accessibility, and other environmental impacts can affect the social and economic lives of residents. For example, residents who depend on agriculture may experience difficulties due to changes in soil and water quality.

Figure 22. Satellite Image of the Research Area in 1985

Figure 23. Satellite Image of the Research Area in 2001

Figure 24. Satellite Image of Research Area in 2013

Figure 25. Satellite Image of Research Area in 2019

Figure 26. Satellite Image of Research Area in 2024

In some of the images above, we can see changes in the landscape from year to year in the research area of Bukit Batu Putih and its surroundings. Changes in the landscape due to human activities, as shown in the DEMNAS 1915-41_v1.0 map and the results of orthophoto acquisition, show a broad impact on the physical and social environment. Mining activities that change the peak of Bukit Batu Putih from an area with many steep slopes to wider plains and gentler slopes illustrate how human intervention can drastically change *the landscape*. These impacts include soil erosion and degradation, hydrological changes, habitat loss, geological stability, microclimate changes, and significant social and economic impacts. Therefore, it is important to carry out good environmental planning and management so that the negative impacts of landscape changes can be minimized.

CONCLUSION

The study identified limestone as the dominant mineral with good quality, with mining activities taking place in the area. Limestone is spread lengthwise along strike from north to south, with varying layer thicknesses, indicating significant potential for exploitation. Four main limestone layers were identified: LM-04 (1.60 meters), LM-03 (8.70 meters), LM-02

(49.0 meters), and LM-01 (12.72 meters). This limestone is included in the Pulau Balang Formation which was formed in the Middle Miocene. The total limestone resources are estimated to reach 18,762,655 cubic meters. Limestone with high calcite content has various industrial applications, such as cement production, increasing the pH of acidic soils, lime and soda ash production, as well as fillers and coatings in paper, stabilizers in glass production, fluxes in the metal industry, and fillers in consumer products. With large resource estimates and good quality, the limestone in Bukit Batu Putih has significant economic value and is worthy of further exploitation.

The limestone in Bukit Batu Putih has significant economic potential and can be exploited for various industries, supported by accurate mapping technology and comprehensive geological understanding, enabling sustainable and effective natural resource management.

BIBLIOGRAPHY

Barbier, E. (2019). *Natural resources and economic development*. Cambridge University Press.

Derbyshire, E. (2019). *Geomorphological processes*. Routledge.

Dikshit, A., Sarkar, R., Pradhan, B., Acharya, S., & Alamri, A. M. (2020). Spatial landslide risk assessment at Phuentsholing, Bhutan. *Geosciences*, *10*(4), 131. https://doi.org/10.3390/geosciences10040131

Eneh, C. A., & Nnenwa, M. (2022). Soil Erosion and Soil Degradation: Conceptual, Theoretical and Panacea Study. *Sustainable Human Development Review*, *14*(1–4).

Goudie, A. S. (2016). Quantification of rock control in geomorphology. *Earth-Science Reviews*, *159*, 374–387. https://doi.org/10.1016/j.earscirev.2016.06.012

Green, D. R., Hagon, J. J., Gómez, C., & Gregory, B. J. (2019). Using low-cost UAVs for environmental monitoring, mapping, and modelling: Examples from the coastal zone. In *Coastal management* (pp. 465–501). Elsevier. https://doi.org/10.1016/B978-0-12-810473-6.00022-4

Hack, H. R. G. K. (2020). Weathering, erosion, and susceptibility to weathering. *Soft Rock Mechanics and Engineering*, 291–333.

Huang, F., Liu, K., Li, Z., Zhou, X., Zeng, Z., Li, W., Huang, J., Catani, F., & Chang, Z. (2024). Single landslide risk assessment considering rainfall-induced landslide hazard and the vulnerability of disaster-bearing body. *Geological Journal*, *59*(9), 2549–2565. https://doi.org/10.1002/gj.4976

Huggett, R., & Shuttleworth, E. (2022). *Fundamentals of geomorphology*. Routledge.

Issaka, S., & Ashraf, M. A. (2017). Impact of soil erosion and degradation on water quality: a review. *Geology, Ecology, and Landscapes*, *1*(1), 1–11. https://doi.org/10.1080/24749508.2017.1301053

Lu, M., & Zhao, Y. (2024). Mineral resource extraction and environmental sustainability for green recovery. *Resources Policy*, *90*, 104616. https://doi.org/10.1016/j.resourpol.2023.104616

Morino, C., Coratza, P., & Soldati, M. (2022). Landslides, a key landform in the global geological heritage. *Frontiers in Earth Science*, *10*, 864760.

Mujiyo, M., Hardian, T., Widijanto, H., & Herawati, A. (2021). Effects of land use on soil degradation in Giriwoyo, Wonogiri, Indonesia. *Journal of Degraded and Mining Lands Management*, *9*(1), 3063. https://doi.org/10.15243/jdmlm.2021.091.3063

Pessacg, F., Gómez-Fernández, F., Nitsche, M., Chamo, N., Torrella, S., Ginzburg, R., & De Cristóforis, P. (2022). Simplifying UAV-based photogrammetry in forestry: How to generate accurate digital terrain model and assess flight mission settings. *Forests*, *13*(2), 173. https://doi.org/10.3390/f13020173

Putra, N. R., Yustisia, Y., Heryanto, R. B., Asmaliyah, A., Miswarti, M., Rizkiyah, D. N., Yunus, M. A. C., Irianto, I., Qomariyah, L., & Rohman, G. A. N. (2023). Advancements and challenges in green extraction techniques for Indonesian natural products: A review. *South African Journal of Chemical Engineering*, *46*(1), 88–98.

Rudiarto, I., Rahmawati, I., & Sejati, A. W. (2020). Land degradation and community resilience in rural mountain area of Java, Indonesia. *Gully Erosion Studies from India and Surrounding Regions*, 449–460.

Saleh, H., Surya, B., Annisa Ahmad, D. N., & Manda, D. (2020). The role of natural and human resources on economic growth and regional development: With discussion of open innovation dynamics. *Journal of Open Innovation: Technology, Market, and Complexity*, *6*(4), 103. https://doi.org/10.3390/joitmc6040103

Singh, M., & Hartsch, K. (2019). Basics of soil erosion. In *Watershed Hydrology, Management and Modeling* (pp. 1–61). CRC Press.

Wang, Y., & Nanehkaran, Y. A. (2024). GIS-based fuzzy logic technique for mapping landslide susceptibility analyzing in a coastal soft rock zone. *Natural Hazards*, 1–33.

Youssef, Y. M., Gemail, K. S., Sugita, M., AlBarqawy, M., Teama, M. A., Koch, M., & Saada, S. A. (2021). Natural and anthropogenic coastal environmental hazards: An integrated remote sensing, GIS, and geophysical-based approach. *Surveys in Geophysics*, 1–33.

Zondervan, J. R., Stokes, M., Boulton, S. J., Telfer, M. W., & Mather, A. E. (2020). Rock strength and structural controls on fluvial erodibility: Implications for drainage divide mobility in a collisional mountain belt. *Earth and Planetary Science Letters*, *538*, 116221. https://doi.org/10.1016/j.epsl.2020.116221